JTD
ISSN 1346-7824
www.jtdweb.org
Institute of Acoustics

7TH INTERNATIONAL SYMPOSUM ON TEMPORAL DESIGN
JOINT WITH JASTICE ANNUAL MEETING
TOKYO 24-25 NOVEMBER 2015

Time-dependent Behavior of Cold-rolled Steel Columns at High Temperatures

Clara María ALVAREZ GONZÁLEZ[a] and Takeshi OKABE[a]

[a] Graduate School of Science and Technology, Kumamoto University, 2-39-1 Kurokami Chuou-ku, 860-8555 Kumamoto, JAPAN, e-mail: clara_al@yahoo.com

ABSTRACT

The mechanical behavior of cold-rolled square steel columns under fire conditions is discussed. In particular, an identification method of creep behavior model for structural steel at high temperature is proposed. In this study, laboratory tests were performed on BCR295 columns as well as numerical simulations with shell elements S4R using the nonlinear finite-element procedure ABAQUS. The success of analyzing the behavior of steel structures under fire conditions depends on how accurately time dependent mechanicals properties can be predicted in the range 500^{o}C ~700^{o}C. The material constants of creep in power-law form were predicted from a limited set of constant strain-rate tested data of stub-columns at high temperatures. It is possible to predict creep flow behavior of metals based on a few stress-strain tests (tensile or compression tests) and using a fundamental equation relating stress, strain rate and temperature and determination of relevant constants. Comparing the results of ABAQUS analysis and the column test data at high temperatures, it was shown that the material constants for calculating creep strain appears to be feasible for predicting the time-dependent behavior of BCR295 steel columns at high temperatures.

1. INTRODUCTION

Cold-rolled steel members have been widely used in various buildings as primary load-bearing columns in Japan. Column buckling at elevated temperatures is one of the most significant causes of collapse for steel frames subjected to fire. Therefore, it is important to examine the compression behavior of cold- rolled steel columns at elevated temperatures.

2. STUB-COLUMN TESTS OF COLD-ROLLED BOX COLUMNS

In Ref.[1], an experimental study was conducted by the author to evaluate the effects of high temperatures and loading rate on the compression behavior of cold-rolled steel box stub-columns.

Testing Setup and Test Program

Figure 1 shows a general view of the test setup. The stub-columns SHS-100x100x9 were 450-mm in length and made of cold-rolled BCR295 (Japanese Standard). All tests were steady-state temperature compression tests at room temperature and four different temperatures: 400°C, 500°C, 600°C, and 700°C. These tests were conducted using two different displacement-controlled loading rates: 0.1 %/ minute and 1.0 %/ minute.

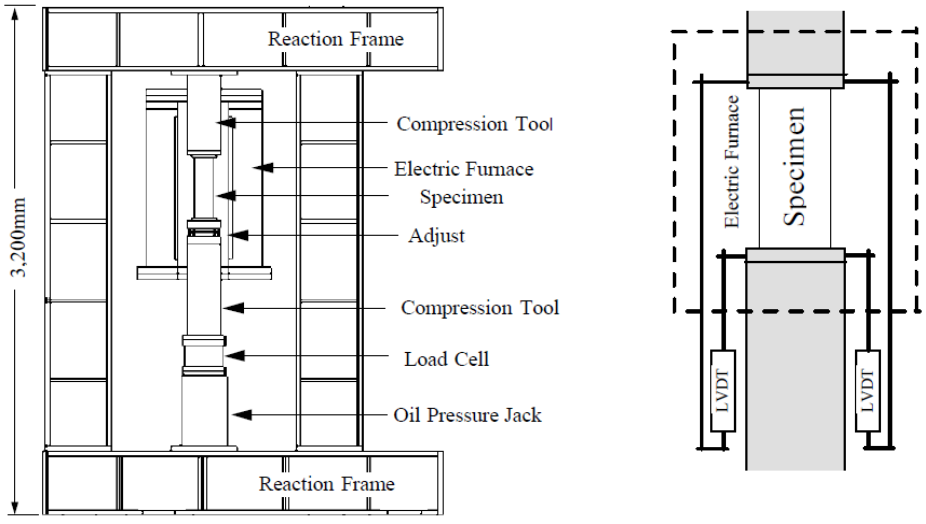

Figure 1. Schematic diagrams of loading assembly and set-up in the furnace and specimen.

Tests Results and Elastic-Plastic Analysis by ABAQUS

Figure 2 shows the distribution of temperatures at various positions along a specimen and load-displacement curves of stub-column tests. Load-displacement curves are shown by the average stress in section as a function of the axial average strain. The solid and dashed lines

indicate the rate of induced column contraction: 1%/minute (FAST tests) and 0.1%/minute (SLOW tests), respectively.

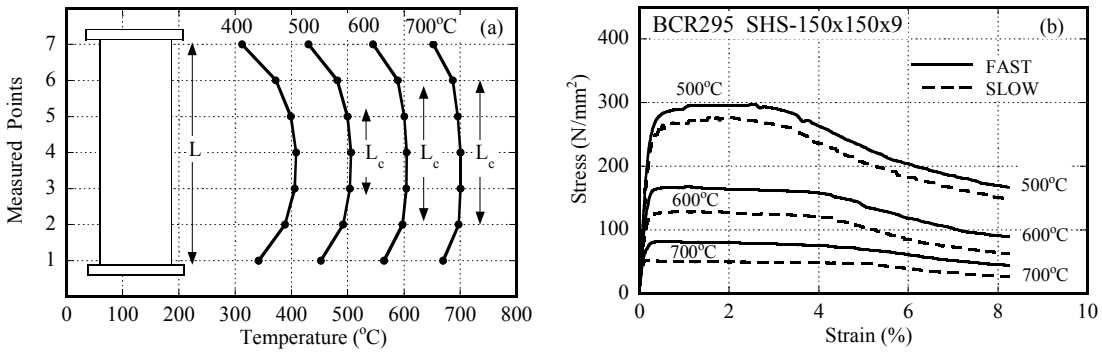

Figure 2. Temperature distribution (a) load-displacement curves, (b) tested.

The ultimate loads of the columns decreased with a temperature increase and due to the rate dependency at high temperatures. The ultimate loads of FAST tests are higher than those of SLOW tests at 500°C ~700°C.

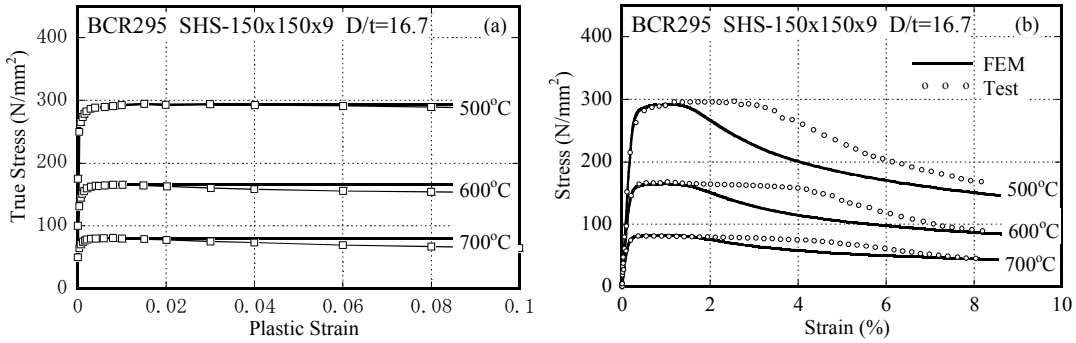

Figure 3. (a) Stress vs. plastic-strain curves and (b) load-displacement curves of stub-columns

Elastic-plastic analyses by the nonlinear finite-element procedure ABAQUS were carried out to simulate the behavior of stub-columns at elevated temperatures, and the results were compared with those derived from current experimental works[1]. The specimens were modeled using shell elements with four nodes per element (S4R type).

In Figure 3, the true-stress and plastic-strain curves at elevated temperatures used in the analysis are shown: load-displacement curves of stub-columns with the results of the compression test (circles) and those of the finite-element analyses (solid lines). The deformation capacity of time-independent (elastic-plastic) analysis at high temperatures is significantly smaller than that in the experimental results.

3. CREEP MODEL FOR BCR295 STEEL AT HIGH TEMPERATURE

The success of analyzing the behavior of steel structures under fire conditions depends on how accurately time-dependent mechanicals properties can be predicted in the range 500^{o}C ~700^{o}C. In this study, a creep behavior model and the identification methodology of material constants for the creep model at high temperature are shown.

Correlation of creep and constant strain rate behavior

T. NEERAJ et al. [2] made one attempt to correlate the constant strain rate behavior and primary creep in metals, and derived analytical result from which one can predict creep behavior from the analysis of constant strain rate tests in titanium alloys at room temperature.

In an empirical analysis, the Holloman flow equation is assumed for the constant strain rate behavior:

$$\sigma = K\varepsilon_p{}^n \dot{\varepsilon}_p{}^m \tag{1}$$

where K is the strength parameter, n is the strain-hardening exponent, and m is the strain-rate sensitivity exponent. This equation was suggested to describe some Ti-alloy behavior [2]. Thus, they show:

$$\dot{\varepsilon} = \frac{d\varepsilon}{dt} = \left(\frac{\sigma}{K}\right)^{1/m} \cdot \varepsilon^{-n/m} \tag{2}$$

$$\int \varepsilon^{n/m} d\varepsilon = \int \left(\frac{\sigma}{K}\right)^{1/m} dt \tag{3}$$

under constant stress,

$$\varepsilon = \left(\frac{\sigma}{K}\right)^{\frac{1}{m+n}} \cdot \left(\frac{m+n}{m}\right)^{\frac{m}{m+n}} \cdot t^{\frac{m}{m+n}} \tag{4}$$

This equation is equivalent with the power-law form:

$$\varepsilon_p = A\sigma^B t^C \tag{5}$$

where

$$A = \left(\frac{1}{K}\right)^{\frac{1}{m+n}} \left(\frac{m+n}{m}\right)^{\frac{m}{m+n}}, \quad B = \frac{1}{m+n}, \quad C = \frac{m}{m+n} \tag{6}$$

The equations (1) to (6) show the correlation of creep and constant strain rate behavior.

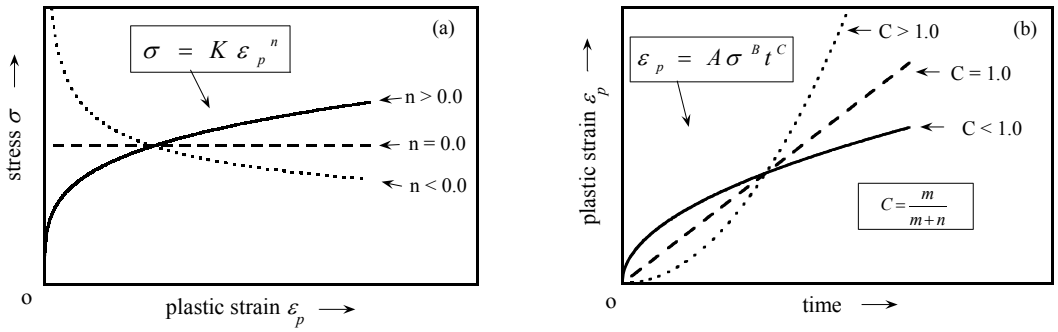

Figure 4. Schematic diagram illustrating a relation between tensile (a) and creep (b) behavior.

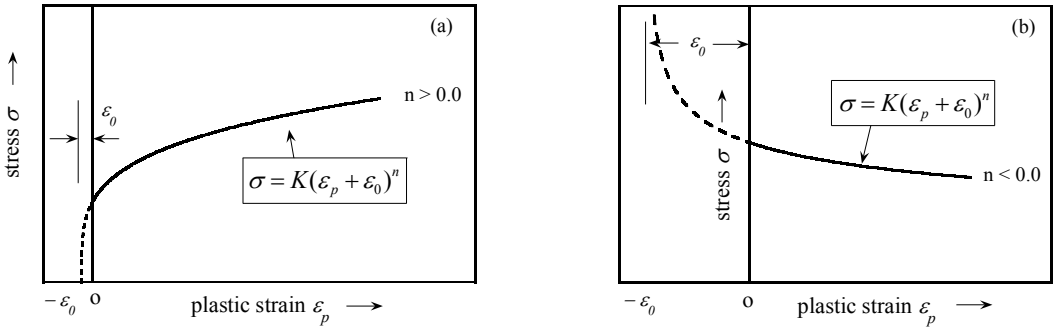

Figure 5. Offset stress vs. plastic strain curves for $n > 0.0$ (a) and $n < 0.0$ (b).

Although, in Ref.[2] the strain-hardening exponent n in Eq.(1) was limited to be positive value, in this research the value of n was generalized to the region of negative value in order to express strain-softening behavior given by Eq.(1). In order to illustrate how the shapes of constant strain rate behave (Eq. (1)), and creep curves (Eq. (5)) change with the values of material constants n and C, the schematic diagrams are shown in Figure 4. The three creep curves shown in Figure 4(b) are dominated by primary, secondary and tertiary creep type: the C exponent for the primary creep is less than one (decreasing strain rate), for the secondary creep is one (constant strain rate), and, for the tertiary creep is greater than one (increasing strain rate).

Moreover, as shown in Figure 5, the constant strain rate behavior (Eq.1) is offset to plastic strain to fit the experimental data reasonably well.

As it can be seen in Figure 2 (a), the higher temperature is distributed over the central part of a stub-column specimen, the time-dependent plastic strain (creep strain) is assumed to concentrate along the length L_c in the stub-column specimen. In order to decide the strain-rate sensitivity exponent m, the real strain rate of model is calculated considering the ratio of length L and L_c (Table 1).

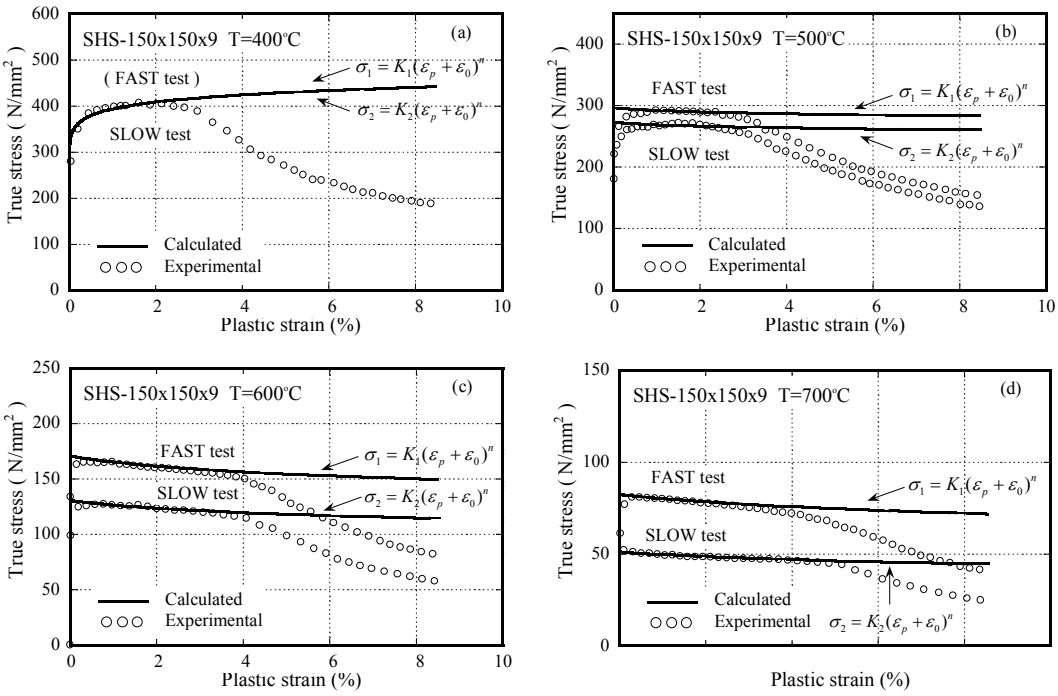

Figure 6. Fitted curve of true plastic strain vs true stress of BCR295 constant strain rate data.

The curves represented by the solid lines in Figure 6 show the flow curves of the material at two strain rates (FAST and SLOW). Strain hardening exponent *n* was not affected by any strain rate. The flow curves at different strain rates appeared to be expressed appropriately by the Holloman flow equation with the strain hardening exponent *n*. This fact indicates that *n* does not vary strongly with strain rate.

Table 1. Material constants for Holloman flow equation and power-law creep curve

°C	K_1	K_2	n	ε_0	L_c/L	K	m	A	B	C
400	505.0	500.0	0.054	0.00	1.00	517.0	0.005	1.38E-46	16.93	0.09
500	270.0	248.4	-0.020	0.01	0.36	314.3	0.042	3.5E-115	45.61	1.91
600	125.0	95.6	-0.080	0.02	0.60	218.4	0.135	1.81E-44	18.29	2.46
700	56.0	34.7	-0.120	0.04	0.64	154.4	0.240	1.64E-19	8.31	2.00

The assumed Holloman parameters for BCR295 are tabulated in Table 1. Values of *m* listed in Table 1 were determined based on the measured material constants K_1 and K_2. The creep parameters *A*, *B* and *C* were calculated by Eq.(6). These material constants data are summarized in Table 1.

Based on these relations, creep behavior in cold-rolled steel at high temperatures can be predicted from a limited set of constant strain-rate data at high temperatures. It appears that

one can predict the creep response of BCR295 reasonably well from constant strain rate data. This is clearly useful considering that the constant strain rate experiment can be accomplished rapidly compared with a set of creep experiments.

4. SIMULATION OF THE TIME-DEPENDENT BEHAVIOR OF COLUMNS

Computational predictions of stub-column tests were carried out using the finite element software ABAQUS [3]. The creep model of BCR295 was implemented in an ABAQUS subroutine. Both, the temperature dependency and strain-rate sensitivity of the material parameters have been examined by the analysis of stub-columns tests at high temperatures. All the models simulated the steady-state temperature compression tests, in which columns were first heated to the target temperature under no load and then compressed under uniform temperature conditions. The simulations were accomplished by the displacement-control method in which the resulting axial load of the columns was computed by specifying the value of the forced axial contraction.

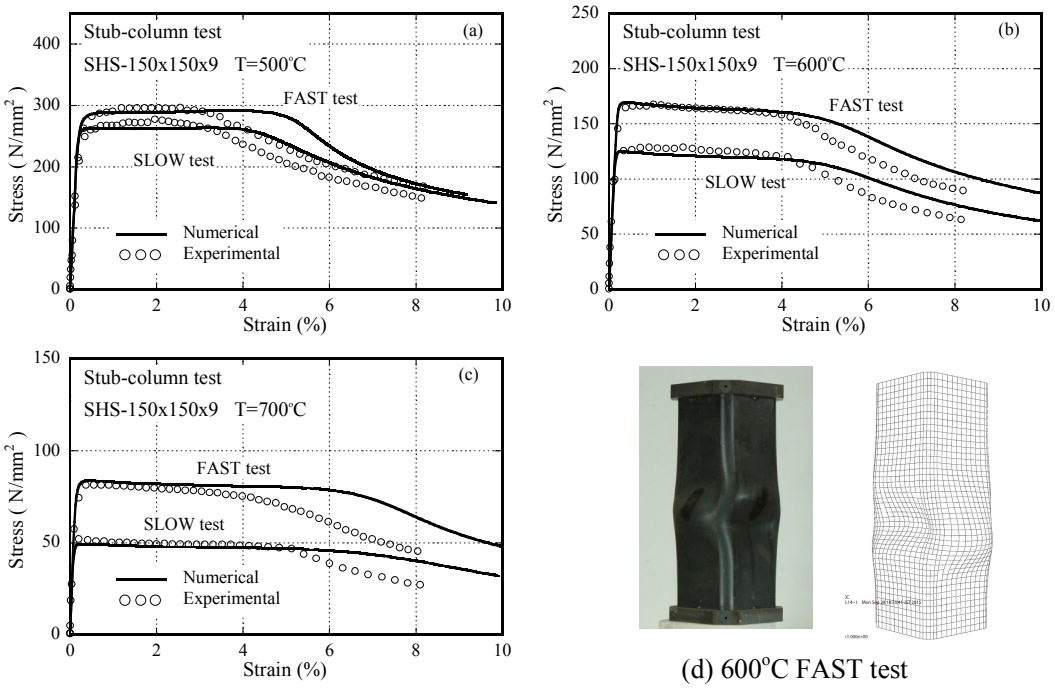

(d) 600°C FAST test

Figure 7. Experimental and numerical axial load-displacement curves for (a) 500°C, (b) 600°C, (c) 700°C, a*n*d (d) deformed specimens after tests.

Figure 7 shows the comparison of experimental (dotted lines) and numerical (solid lines) axial load-displacement curves for (a) 500°C, (b) 600°C, (c) 700°C. Deformed specimens after 600°C tests are shown in (d): laboratory tested specimen on the left and ABAQUS simulated specimen on the right.

Figure 7 shows that the numerical procedure approximately reproduced both, the profile of the load-deflection curves at different strain rates and the delay of the unloading of axial-load at high temperatures.

5. CONCLUSIONS

Based on the use of the strain-rate-sensitivity Holloman flow law, it has been shown that one can predict reasonably well the time-dependent response of cold-rolled steel BCR295 at high temperatures from a limited set of constant strain rate data for materials. This is clearly useful considering that the constant strain rate experiment can be accomplished rapidly compared with a set of creep experiments. The effect of loading rate on the deformation behavior of stub-column tests was examined and the significance of employing a creep models at high temperatures was discussed and some of their limitations were evaluated.

6. REFERENCES

[1] Y. Kuroiwa, T. Ave and T. Okabe, "Compression Behavior of Cold-Formed Steel Box Stub-Columns at High Temperature", Proceedings of the 9th Pacific Structural Steel Conference 2010, China, 2010, pp. 1114-1120.

[2]Y. Neeraj, D.-H. Hou, G. S. Daehn and M. J. Mills, "Phenomenological and Microstructural Analysis of Room Temperature Creep in Titanium Alloys", Acta Materialia, Vol. 48, 2000, pp. 1225-1234.

[3] Dassault Systèmes Simulia Corp., "Abaqus 6.14 Documentation Collection" , Providence, RI, USA., 2014, http://abaqus.software.polimi.it/v6.14/index.html